

Recent Trends and Challenges in Welding of Automotive Steels

Murugaiyan Amirthalingam

Assistant Professor, Head, Joining and Additive Manufacturing Laboratory,
Dept. of Metallurgical and Materials Engineering, Indian Institute of Technology, Madras, Chennai, India.
Email: murugaiyan@iitm.ac.in

DOI : 10.22486/iwj.v53i2.195582

Abstract

The development of modern automotive vehicles with improved environmental, safety and vehicle performance has driven the development of new steel grades that are lighter, safer, greener and more cost effective. As a result, conventional low carbon steels and high strength steels are increasingly replaced with advanced high strength steels (AHSS) due to their high strength and good uniform elongation. This unique combination in mechanical properties is achieved by carefully designing the microstructure by adding special alloying elements and controlled heat treatments. In automotive manufacturing processes, fusion welding is an important process employed for the joining of steel parts and components. However, the thermal cycle of a welding process destroys the carefully designed microstructure of AHSS. In order to use these materials effectively, it is necessary to have a sound understanding of the influence of weld thermal cycles and alloying additions on the evolution of microstructure in the fusion and heat affected zones. In this paper, the current understanding and recent developments in the welding of current generation advanced high strength steels for automotive applications are discussed. The paper concludes with the assessments and possible solutions to improve the weldability of advanced high strength steels for automotive applications.

Keywords: Welding; automotive steel; advanced high strength steel; AHSS; weldability.

1.0 Introduction

The implementation of Bharath VI emission norms necessitates the use of lighter, stronger and safer materials in place of conventionally used alloys to produce automotive components. Significant reduction in weight of an automotive vehicle is required to meet the stringent emission target (**Fig. 1**), however without compromising crashworthiness, passenger safety and comfort [1].

Significant efforts are made to replace steel with aluminium, magnesium alloys and carbon fibre reinforced plastics (FRP) to produce light-weight automotive parts. However, the inherent manufacturing challenges to produce high strength aluminium, magnesium alloys and composite materials limit their use to produce automotive components. Moreover, the net greenhouse gas emission during the primary production of steel is still by far lower than aluminium, magnesium and carbon FRP composite materials (**Fig. 2**). Therefore, steel is

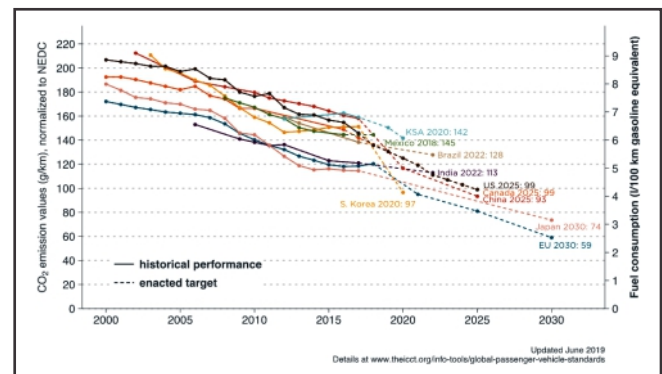


Fig. 1: Passenger car CO₂ emission and fuel consumption values, normalised to New European Driving Cycle [1].

still considered as a best material to produce light-weight automotive parts and components [2]. Efforts are made over last two decades to develop new generation of automotive

steels, commonly known as advanced high strength steels (AHSS) which possess high strength and excellent uniform elongation. The first and second generation of AHSS family include Dual Phase (DP), Complex-Phase (CP), Ferritic-Bainitic (FB), Martensitic (MS), Transformations Induced Plasticity (TRIP) and Hot-Formed (HF) steels. These steels possess ultimate tensile strength in the range of 600 to 1000 MPa with a total elongation of 15 to 40 % [2].

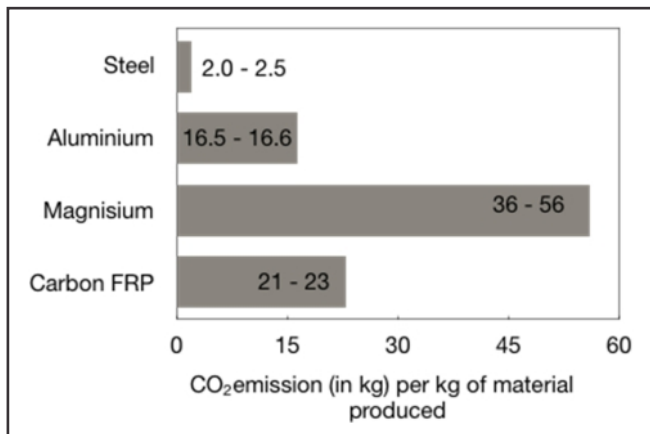


Fig. 2 : Current average greenhouse gas emissions from primary production in kg CO₂ emission per kg of material [2].

The combination of high strength and excellent uniform elongation is achieved by alloying strategies in combination with carefully controlled thermomechanical processing methodologies to produce multi-phase containing microstructures in AHSS. Although several alloying strategies for these steels exist, most of them have relatively high levels of carbon (up to 0.2 wt. %), manganese (up to 2 %), silicon (up to 1.5 wt. %), aluminium (up to 1 %) and sometimes phosphorous (up to 0.08) as compared to conventional automotive steels (deep drawn grade, interstitial free, bake hardening and high strength low alloyed steels)

Modern passenger vehicle designs involve a large number of different steel grades in an effort to maximise the combined advantages these have to offer [2]. In order to realise such a design, there is a need to join these materials in such a way that they can effectively transfer loads without introducing areas of weakness. Ideally, the joints should be stronger than the parent material, whilst having matching properties in terms of toughness and formability. In addition, joints should be durable, the quality should be readily assessable, and the joining process should be suitable for implementation on an industrial scale. Welding is often employed as the best compromise to meet these requirements. One of the significant disadvantages of fusion welding is that the thermal cycle of a welding process destroys the carefully designed microstructure. Local melting and re-solidification during

fusion welding results in an as-cast microstructure, whilst rapid heating and cooling in the heat affected zone leads to significant microstructural changes with respect to the parent materials, resulting in changes in mechanical properties and the development of a new and generally undesirable distribution of stresses.

In this work, an overview of recent advancement made in identifying optimised welding procedures for welding of AHSS is presented, with a special emphasis on the author's recent work on the welding behaviour of dual phase (DP) and transformation induced plasticity (TRIP) steel. A brief description on some of the limitations on our current understanding are highlighted with a view to stimulating future scientific research.

2.0 Background

Steels are commonly classified according to their carbon content [3]. Steels for automotive construction typically contain 0 to 0.25 weight % carbon. The properties of such steels, which always contain some manganese, silicon, phosphorus and sulphur as well as minor amounts of other elements [4], are primarily dependent upon the microstructure and the amount and distribution of carbon present. According to the American Iron and Steel Institute's definition, plain carbon steels may contain up to 1.65 % manganese, 0.60 % silicon and 0.60 % copper in addition to much smaller amounts of other elements [4]. The main influence of these alloying elements is to increase the strength, toughness and hardenability of the steel.

Microstructural homogeneity and low carbon contents ensure that plain carbon steels generally show good formability. Increased strength can be obtained either by cold working, alloying, or adding small quantities of grain refining elements. Cold working increases dislocation density, but its effect on strength is limited by the chemical composition and microstructure of the steel. Alloying increases cost and can lead to weldability problems [5]. The addition of small concentrations (<0.1 wt. %) of grain refining elements such as niobium, titanium and vanadium to steels with 0.03 to 0.08 wt. % C and up to 1.5 wt. % Mn make it possible to produce fine-grained material with yield strengths between 450 and 550 MPa [6]. Low alloyed steels, typically containing manganese and silicon, can exhibit both high strength and good formability if they are heat treated to produce a matrix of body centred cubic ferrite with islands of body centred tetragonal martensite. This structure is characteristic of dual phase (DP) steels, an example of which is shown in **Fig. 3**.

Low alloy TRIP steels always contain manganese and silicon and may have appreciable quantities of aluminium and phosphorous in addition to grain refining elements such as niobium and molybdenum.

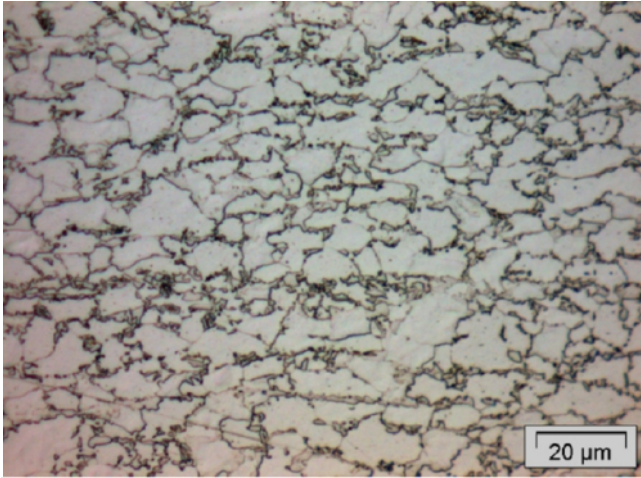


Fig. 3 : A typical dual phase (DP) steel microstructure, showing a ferrite matrix with about 20 % of martensite distributed along the boundaries of ferrite grains.

The primary function of manganese in steel (0.3 to 0.8 wt. %) is to reduce the occurrence of iron-sulphides (which may cause problems during hot rolling of the steel sheets) and oxides. Some excess manganese contributes to carbide formation (Mn_3C), in solid solution with Fe_3C ; the remainder dissolves in the iron matrix. Extra manganese is often added to enable the reduction of the carbon content whilst maintaining tensile strength and improving ductility [6]. Additionally, manganese serves to widen the temperature range over which austenite is stable and thus to depress the austenite to ferrite transformation temperature, which facilitates the formation of retained austenite upon quenching [6, 7, 10].

Silicon is added to steels to "kill" or deoxidise them. Silicon dissolves in the ferrite, raising the strength by solid solution hardening. Silicon is a ferrite stabiliser which acts to restrict the temperature range over which austenite is stable and to promote ferrite grain growth. [6] Silicon retards the precipitation of cementite during bainite formation [11]; hence, during isothermal holding silicon promotes the enrichment of austenite with carbon. A similar outcome can be achieved by replacing some of the silicon with aluminium.

Both manganese and silicon affect the bonding behaviour of the steel with a zinc coating. Hot dip-galvanising of TRIP steel (0.2C, 1.5Mn, 1.5Si) is reported to result in a poor surface quality with bare spots. This is attributed to surface segregation and subsequent oxidation of manganese and silicon, which reduces the wettability of the steel substrate [12].

Aluminium replaces about 1 wt. % of silicon in modern TRIP steels to reduce the adverse effects of surface oxidation, resulting in TRIP steels which are suitable for hot-dip galvanising. Aluminium, like silicon, is insoluble in cementite and retards its formation. Unlike silicon, aluminium is found to

increase the kinetics of bainite formation leading to a reduced austempering time [13]. However, due to the lower solid solution strengthening of aluminium compared with silicon, use of a strong solid solution strengthening element such as phosphorus is required when replacing silicon.

Phosphorus is normally found in solid solution in the ferrite phase and is effective at increasing the strength of a steel. It also functions as a ferrite stabiliser and coarsens the ferrite grain size [14]. In addition, it raises the ductile to brittle transition temperature, leading to decreased fracture toughness; the concentration is therefore often kept at as low as possible. Phosphorus plays an important role in TRIP metallurgy. Its low solubility in iron-carbides significantly retards the formation of cementite where the diffusion of phosphorus away from the carbide becomes the rate determining step. Phosphorus, together with silicon and aluminium are the three elements usually adopted in TRIP steels to ensure that carbon does not precipitate from bainite during isothermal bainitic holding, but diffuses across the growth front to austenite. Phosphorus, whilst being a ferrite stabiliser thus indirectly stabilises austenite in TRIP steels [14]. Although phosphorus is soluble in ferrite, upon rapid solidification (i.e. straight from the weld pool), it tends to segregate on the austenite grain boundaries [14].

The presence of these alloying elements leads the formation of non-metallic inclusions, stabilisation of unwanted phases in the weld zone. Moreover, the segregation of alloying elements in the solidification primary grain boundaries increases the hot cracking susceptibility during welding and brittleness of the welds as described in the following sections.

3.0 Influence of welding on TRIP steel microstructures

The distribution and characteristics of the microstructures obtained when welding TRIP steels depend to a significant extent on the chemistry of the steel and on the details of the imposed weld thermal cycle. Parent material microstructures for a silicon and an aluminium containing TRIP steel is shown in **Fig. 4**. The volume fractions of retained austenite in the parent microstructures are 10 and 11 % respectively.

The fusion and heat affected zones of GTA welded TRIP steels contain primarily a martensitic structure (**Fig. 5**), with about 4 to 5 % retained austenite. The heat affected zones are wider than those observed in other steels due to low temperature austenite transformation. Fusion zones in both silicon and aluminium containing steels show the presence of inclusions, mainly decorating the grain boundaries; those in the aluminium rich steel being smaller on average than those in the silicon rich steel. Inclusion density is found to be greatest in the columnar grain region of the weld and is reduced close to the centre of the weld where a more equi-axed structure is found.

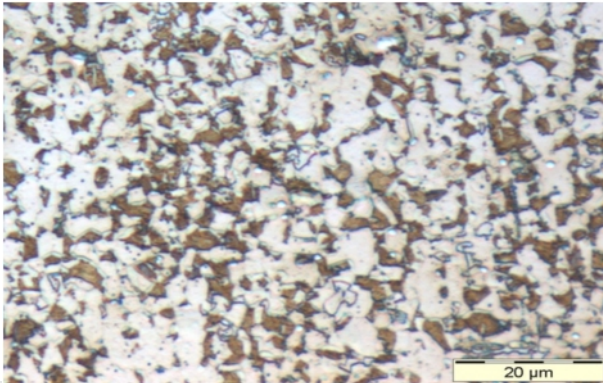


Fig. 4 : A typical TRIP steel microstructure, showing a ferrite matrix with bainite and retained austenite (small bright white regions).

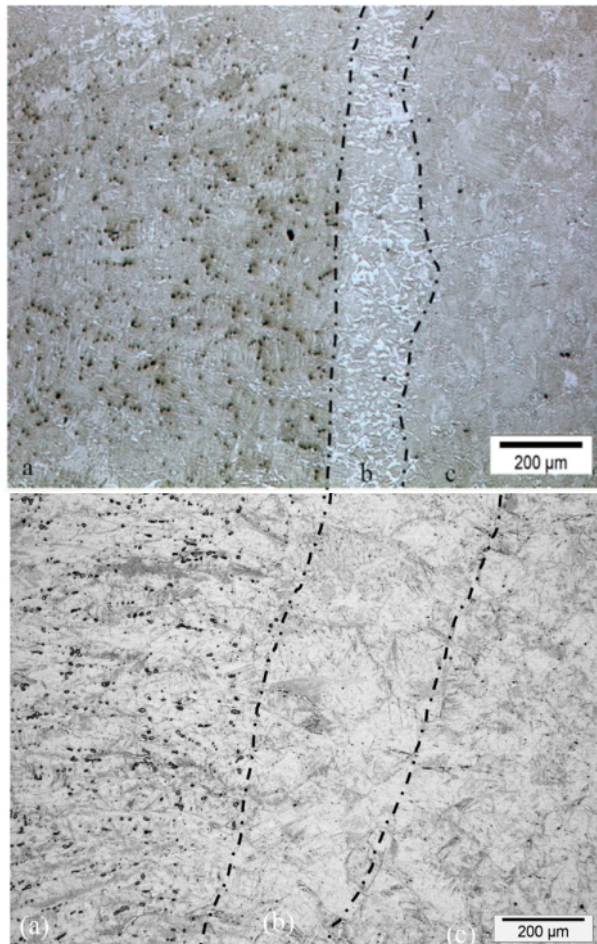


Fig. 5 : Optical micrograph of a weld in (top) an aluminium rich TRIP steel showing (a) inclusions in the fusion zone, (b) a ferritic fusion line and (c) a coarse grained HAZ with grain boundary ferrite; and (bottom) a silicon TRIP steel showing a martensitic structure and the presence of inclusions in (a) the fusion zone. Region (b) is the coarse grained HAZ, and region (c) the fine grained HAZ [15].

These inclusions are detrimental to both the strength and elongation of the welds. A soft band of allotriomorphic ferrite is observed at the fusion line of the aluminium rich steel, varying in width from about 100 to 200μm, which is also detrimental to the strength of the weld.

The morphologies of the inclusions present in the welds made on silicon and aluminium rich steels are shown in **Fig. 6**. Aluminium and silicon are added to the steel to suppress cementite formation and hence to promote carbon enrichment of the austenite. However, these elements readily form oxides during welding, leaving the weld pool partially depleted.

In the silicon rich TRIP steel, energy dispersive X-ray analysis shows a higher silicon concentration in the core as well as at the sides of the oxide inclusions. The relative concentration of manganese is lower than that in the parent material. Similar behaviour in elemental distribution was found for inclusions in the aluminium containing steel. In this case, the formation of aluminium oxides leads to solute entrapment, and subsequent formation of silicon oxides and manganese sulphides, which grow epitaxially when the liquid weld pool cools down below the solidification temperature. The aluminium content is found to be higher in the core of the inclusion. In the case of the silicon rich steel, which contains only silicon as a strong deoxidizing element, the oxides generally form at a lower temperature than those of aluminium, the average size is therefore smaller, of the order 1 to 2 μm in silicon rich steel and 5 to 6 μm in aluminium rich steel.

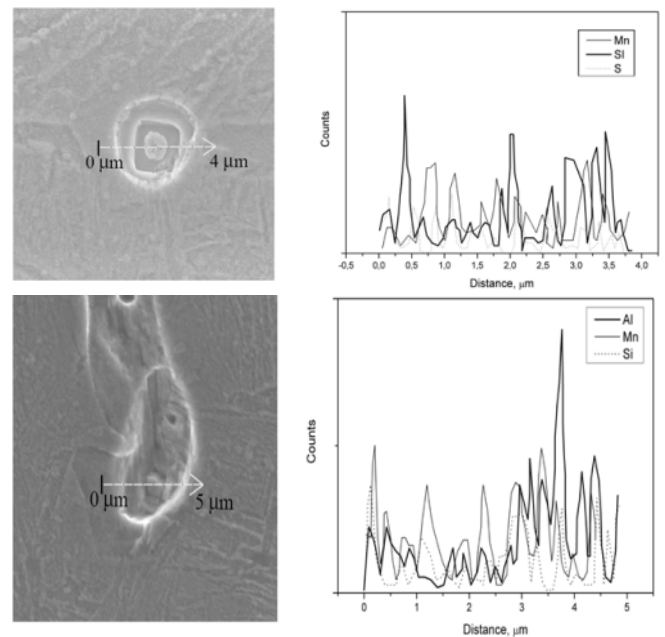


Fig. 6 : Morphology and composition of inclusions in (above) silicon rich and (below) aluminium rich TRIP steels [15].

The ferrite formed at the fusion boundary of the aluminium rich weld has been shown to be enriched with aluminium [15]. Aluminium based TRIP steels, generally contain about 1 to 1.3 wt. % of aluminium. During welding and subsequent solidification of the molten pool, the equilibrium aluminium content in ferrite can rise as high as 1.35 wt. % at 1400 °C for the steel with a bulk aluminium concentration of 1.1 wt. %. According to the corresponding binary Fe-Al phase diagram, if the aluminium content exceeds 1.15 wt. %, ferrite is stabilized. When the liquid weld pool starts to solidify to delta ferrite at the fusion boundaries, aluminium partitions to this ferrite causing stabilization and preventing further transformation into inter-critical austenite and finally to martensite, which would result in a weakened zone at the fusion boundary.

4.0 Elemental segregation and embrittlement of welds

In some AHSS such as transformation-induced plasticity (TRIP) and quench and partitioning (Q&P) steels, phosphorous is added to (i) improve the strength by solid solution strengthening and (ii) reduce the amount of silicon in TRIP and Q&P steels in order to improve the galvanisability. Phosphorous is also known to suppress the formation of cementite and thereby increase the amount of austenite retained at room temperature. However, the segregation of phosphorous to the grain boundaries during welding leads to embrittlement. The formation of complex phosphides affects the amount of substitutional elements in solid solution in the matrix and thereby the hardenability of the steels. The addition of boron to phosphorous containing steels is known to improve grain boundary cohesion by reducing phosphorous segregation, thereby reducing embrittlement.

With a combination of experimental investigation and mathematical modelling, it is shown that addition of boron (about 30 ppm wt. %) can favourably reduce the phosphorous induced weld metal embrittlement [16]. With an acceptable failure mode, tensile peel and cross tension strengths of steel welds are improved with the addition of boron. Boron is found to suppress the grain boundary segregation of phosphorous, thereby reducing the embrittlement of the welds (Fig. 7-8).

The potential challenges regarding brittle weld metal failure in spot welded structures comprising new high strength and higher alloyed AHSS, drive the exploration for dedicated weld schedules, to ensure appropriate mechanical behaviour in car body architectures. For example, the 1.2 GPa AHSS could only be successfully implemented thanks to a dedicated resistance spot weld schedule, developed by the author and his co-workers. In order to design appropriate weld schemes for the AHSS, detailed knowledge of the solidification behaviour, phase transformations, and elemental distributions during welding is required to understand how the weld schedule and

the resulting temperature history affect the final mechanical properties of the resistance spot weld. By using a combination of physical based mathematical modelling and experimental investigations, a unique double pulsing resistance spot welding procedure was developed to reduce weld metal embrittlement and improve the mechanical properties of the AHSS welds [17].

With the combination of finite element and phase field modelling techniques, it is shown that the application of a relatively simple double pulse weld schedule leads to significant improvement of the resistance spot weld failure behaviour and strength during cross tension loading, as compared to welds made with standard single pulse welding. Efforts are now made to develop an inverse approach: first to predict the required weld and post-weld temperature history to minimise segregation of phosphorous based on microstructural modelling and subsequently to employ finite elements models to design the appropriate weld schedule that leads to optimised microstructural properties.

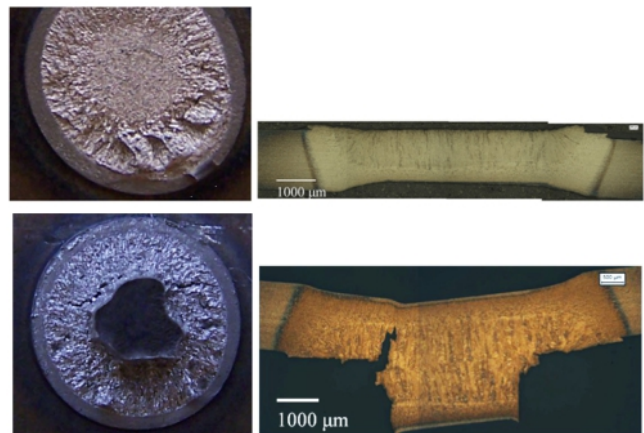


Fig. 7 : Effect of boron addition on the reduction in embrittlement of resistance spot DP steel welds (images on top row shows partial plug failure and failure mode becomes full plug failure with an addition of 30 ppm of boron, bottom row) [16].

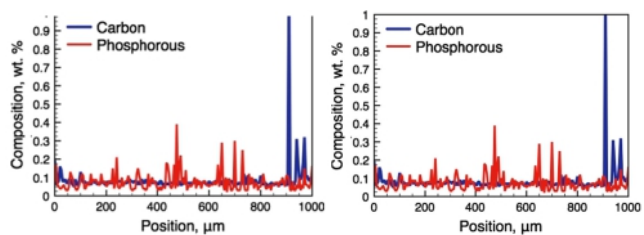


Fig. 8 : Electron probe micro analysis (EPMA) indicates that addition of boron reduced phosphorous segregation in the grain boundaries of DP steel welds [16].

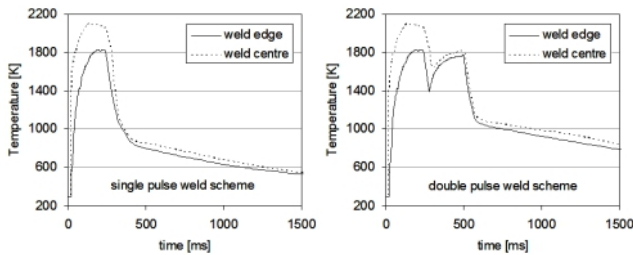


Fig. 9 : A typical conventional resistance spot welding thermal cycle (left) and a novel double pulse weld thermal cycle to reduce elemental segregation in AHSS [17].

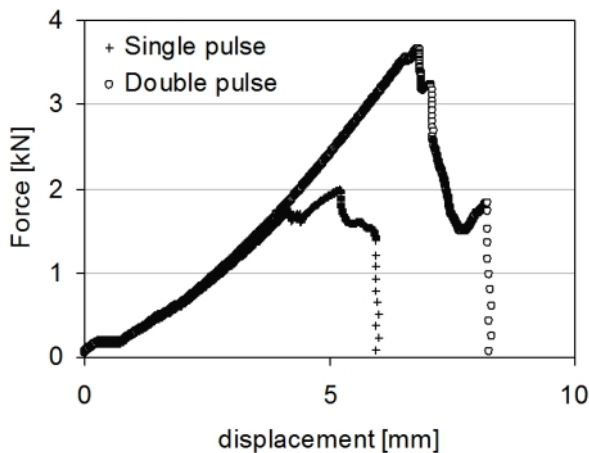


Fig. 10 : Force displacement curve of the cross tension shear tests for single pulse and novel double pulsing resistance spot welding, showing the improvement in mechanical properties [17].

5.0 Hot cracking during welding of AHSS

The higher alloying content in AHSS renders it susceptible to solidification cracking during welding. During weld metal solidification, grains grow perpendicular to the fusion boundary since the temperature gradient is steepest, and accordingly, the heat extraction is maximized. The solidifying dendrites meet at the weld centre line. Upon solidification, the solidifying weld metal shrinks due to solidification shrinkage and thermal contraction. As solidification progresses, the solid in the mushy zone begins to form a rigid continuous network, i.e., tensile strain is induced by the surrounding material. If the deformation exceeds a certain threshold, separation of the dendrites at the grain boundary can occur. At the terminal stage of solidification, such an opening cannot be compensated by the remaining liquid due to both low permeability and a high solid fraction. As a result, solidification cracking occurs. Solidification temperature range, segregation of impurity elements, morphology of solidifying grains, interdendritic liquid feeding and dendrite coherency are some of the important metallurgical aspects affecting the solidification cracking tendency.

A typical car body has 40 m of weld flanges that are welded using resistance spot welding. Resistance spot welding requires 16 mm of the flange width to fit the electrode system on either side. The flange width can be minimized by using laser welding and can lead to an overall weight reduction of up to 30–40 kg [18]. The distance from the free edge at which the welding is carried out is considered important for cracking behaviour in terms of the response of the material to the amount of restraint (Fig. 10). Author and his co-workers carried out extensive investigations using a combined experimental and numerical modelling approach to identify the critical condition as a function of welding distance from the free edge in which no crack occurs in a transformation induced plasticity steel (Fig. 11) [18]. This study provided a vital information to identify the critical location where a weld seam can be placed in during laser welding in overlap configuration in AHSS.

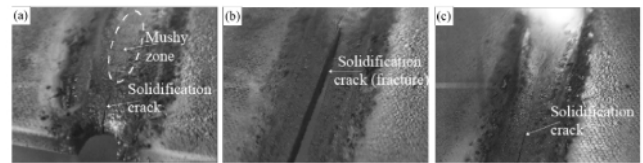


Fig. 11: High speed video images showing (a) onset of solidification cracks during laser welding, (b) complete fracture while welding is carried out close to the edge (5 mm from plate edge) and (c) crack stops propagating further while welding 7 mm from plate edge [18].

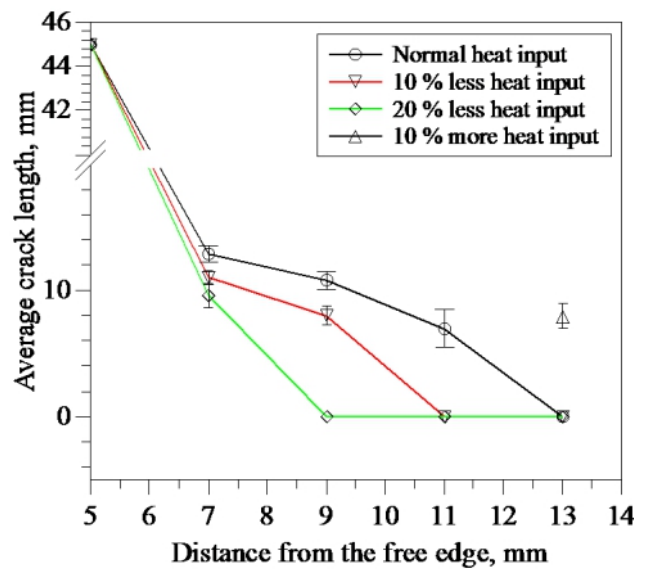


Fig. 12 : Crack length as a function of distance from plate edge during laser welding of a TRIP steel [18].

Author and his co-workers used in-situ high temperature laser confocal microscopy to study the solidification behaviour of a TRIP steel with 0.089 wt. % P. Solidification cracking was observed in the final stages of solidification. Microsegregation of P leads to undercooling resulting in longer and narrower liquid channels that persist in the crack vulnerable region. In addition, P segregation renders the grain boundaries weak. As a result, tensile strain/stress are concentrated at the inter-dendritic boundaries leading to increased susceptibility towards cracking [19].

In order to determine a hot cracking criterion of the tested TRIP steel under the same heat input and constraint condition, a standard self-restraint hot cracking was modified by welding at various locations parallel to the free edge of a steel coupon. The crack susceptibility decreases when welding is performed at a larger distance from the free edge. The critical strain for the onset of hot cracking in the TRIP steel examined was found to be in the range of 3.2 to 3.6% [20, 21].

It is found that the hot cracking susceptibility of TRIP steel is always higher than DP steel, under the same heat input and mechanical constraints, due to presence of increased amount of phosphorous in TRIP steel. The TRIP steel has a broader solidification range than the DP steel. When the dendritic tips coalesce with the weld centre line, the TRIP steel shows a higher pressure drop for the solidification shrinkage and deformation contribution, which explains why the TRIP steel is more susceptible to hot cracking than the DP steel when solidification is nearly complete [22].

The phosphorus concentration is predicted at grain boundary up to 0.55% for the TRIP steel, which is six times higher than the concentration in the base material (0.08 wt. % of P). Segregation of phosphorus can lead to brittle structures at the grain boundary, which increases the hot cracking susceptibility during solidification as a result of thermally induced tensile stress [22].

Author and his co-workers used in-situ high temperature laser confocal microscopy to understand the solidification behaviour of DP and TRIP steels. Liquid feeding and back filling were observed in the inter-dendritic regions during the terminal stages of solidification only in DP steel welds. An average liquid flow speed of 450–500 $\mu\text{m s}^{-1}$ was found. A pressure difference of the order of 104 Pa is calculated to cause the liquid flow. The rate of solidification shrinkage and the rate of deformation were found to be less than the rate of liquid feeding. Conversely, no back-filling was observed in TRIP steel welds which lead to the stabilisation and coalescence of cracks formed during the terminal stages of solidification [23].

6.0 Summary and future research

The stringent emission norms and improved passenger safety concerns drive the development of advanced high strength

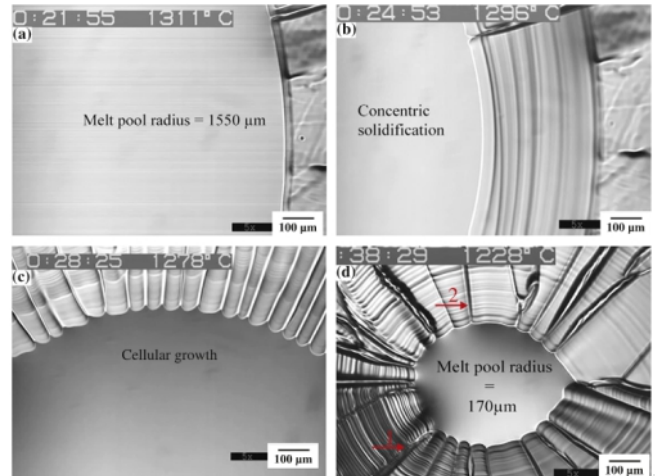


Fig. 13 : In-situ high temperature laser confocal microscopy images showing (a) a stable melt pool of radius 1550 μm is formed to begin with. Afterwards a constant cooling rate of 5 K min^{-1} is applied, (b) solidification progresses in a concentric manner, (c) planar growth changes to cellular, (d) melt pool of radius 170 μm when liquid feeding in the inter-cellular regions was observed. Temperature indicated in images (a–d) is measured at the periphery of the platinum holder. Based on calibration the actual temperature is $\sim 210 \text{ K}$ higher [23].

steels for modern automotive vehicle production. Fusion welding of AHSS with ultimate tensile strength in the range of 600 to 1000 MPa is still challenging due to the (i) formation of non-metallic inclusions, (ii) formation of unwanted phases in the weld zone (iii) embrittlement of welds by elemental segregation and (iv) hot cracking during welding. It is possible to improve the weldability of these automotive steels by understanding the elemental segregation behaviour of alloying elements, alloying strategy and modifying the conventional welding procedure. By using a combination of mathematical modelling and experimental investigations, it is possible to identify the fundamental mechanism by which solidification cracking is observed in these steels. Using the results of this investigation, a safe welding procedure can be formulated to weld these advanced high strength steels for automotive applications. However, the challenge still remains when new grades of automotive steels with strength levels beyond 1000 MPa are to be welded to meet the future emission norms.

Acknowledgment

This paper contains a lot of published information from the author and his co-workers, available in open literatures. Author thanks his co-workers, from Delft University of Technology, the Netherlands, Tata Steel in IJmuiden, the Netherlands and Indian Institute of Technology Madras, India and funding agencies, (i) Materials Innovation Institute (M2i), the Netherlands and FOM, the Netherlands, Department of Science and Technology (DST) and Tata Steel – Europe.

References

- [1] The International Council on Clean Transportation (2019); Global Passenger Vehicle Standards, Vol. June. Web: www.theicct.org/info-tools/global-passenger-vehicles-standards
- [2] Advanced High Strength Steels Application Guidelines (2017); Version 6.0, April 2017, pp.1-7.
- [3] Porter DA, Easterling KE and Sherif MY (2008); Phase Transformations in Metals and Alloys; 3rd edition, CRC press.
- [4] McGannon HE (1971); The Making, Shaping and Treating of Steel, 9th edition, United States Steel.
- [5] Easterling KE (1992); Introduction to the Physical Metallurgy of Welding, 2nd Ed., Butterworth Heinemann.
- [6] Honeycombe R and Bhadeshia HKDH (1995); Steels—Microstructure and properties, 2nd edition, Edward Arnold.
- [7] Hulka K (2003); Modern multi-phase steels for the automotive industry, Materials Science, Testing and Informatics, Materials Science Forum, 414-415, pp.101-110.
- [8] Zackay VF, Parker ER, Fahr D and Busch R (1967); Enhancement of ductility in high-strength steels, ASM Trans. Quart., 60, pp.252-259.
- [9] Tang Z-Y, Ding H, Du L-X, Ding H and Zhang X (2007); Effect of thermomechanical processing on microstructures of TRIP steel, Journal of Iron and Steel Research International, 14(2), pp.56-60.
- [10] Wolk Van Der P (2001); Modelling CCT diagrams of engineering steels using neural networks, PhD Thesis, TU Delft. Web: <http://repository.tudelft.nl/>
- [11] Chatterjee S, Murugananth M and Bhadeshia HKDH (2007); δ TRIP steel, Materials Science and Technology, 23(7), pp.819-827.
- [12] Mahieu J, Claessens S and Cooman De B (2001); Galvanizability of high-strength steels for automotive applications, Met. Trans. A, 32, pp.2905-2908.
- [13] Garcia-mateo C, Caballero FG and Bhadeshia HKDH (2003); Acceleration of low- temperature bainite, ISIJ International, 43, pp.1821–1825.
- [14] Uijl Den NJ and Smith S (2006); Resistance spot welding of advanced high strength steels for the automotive industry, Proceedings of the 4th International Seminar on Advances in Resistance Welding, Wels, Austria.
- [15] Amirthalingam M, Hermans MJM and Richardson IM (2009); Microstructural development during welding of silicon- and aluminum-based transformation-induced plasticity steels-inclusion and elemental partitioning analysis, Metallurgical and Materials Transactions A-Physical Metallurgy and Materials Science, 40A(4), pp.901-909.
- [16] Amirthalingam M, Der van EM, Kawakernaak C, Hermans MJM and Richardson IM (2015); Elemental segregation during resistance spot welding of boron containing advanced high strength steels, Welding in the world, 59 (5), pp.743-755.
- [17] Der van EM, Amirthalingam M, Winter J, Hanlon DN, Hermans MJM, Rijnders M and Richardson IM (2016); Improved resistance spot weldability of 3rd generation ultra high strength automotive steels, Mathematical Modelling of Weld Phenomena, Vol.11, pp.175-194. ISBN 978-3-85125-490-7.
- [18] Agarwal G, Gao H, Amirthalingam M and Hermans MJM (2018); Study of solidification susceptibility during laser welding in an advanced high strength automotive steel, Metals, 8 (9).
- [19] Agarwal G, Kumar A, Amirthalingam M, Moon SC, Dippenaar RJ, Richardson IM and Hermans MJM (2018); Study of solidification cracking in a transformation induced plasticity-aided steel, Mat. Mat. Trans. A, 49(4), pp.1015-1020.
- [20] Gao H, Agarwal G, Amirthalingam M, Hermans MJM and Richardson IM (2018); Investigation on hot cracking during laser welding by means of experimental and numerical methods, Welding in the World, 62, pp.71-78.
- [21] Agarwal G, Gao H, Amirthalingam M and Hermans MJM (2018); In-situ strain investigation during laser welding using digital image correlation and finite-element-based numerical simulation, Science and Technology of Welding and Joining, 23(2), pp.134-139.
- [22] Gao H, Agarwal G, Amirthalingam M and Hermans MJM (2018); Hot cracking investigation during laser welding of high-strength steels with multi-scale modelling approach, Science and Technology of Welding and Joining, 23(4), pp.287-294.
- [23] Agarwal G, Amirthalingam M, Moon SC, Dippenaar RJ, Richardson IM and Hermans MJM (2018); Experimental evidence of liquid feeding during solidification of a steel, Scripta Materialia, 146, pp.105-109.